BIOCHEMISTRY
including biophysical chemistry & molecular biology

Article

pubs.acs.org/biochemistry

Asparagine Repeat Peptides: Aggregation Kinetics and Comparison with Glutamine Repeats

Xiaomeng Lu[†] and Regina M. Murphy*[,‡]

[†]Biophysics Program and [‡]Department of Chemical and Biological Engineering, University of Wisconsin-Madison, Madison, Wisconsin 53706, United States

Supporting Information

ABSTRACT: Amino acid repeat runs are common occurrences in eukaryotic proteins, with glutamine (Q) and asparagine (N) as particularly frequent repeats. Abnormal expansion of Q-repeat domains causes at least nine neurodegenerative disorders, most likely because expansion leads to protein misfolding, aggregation, and toxicity. The linkage between Q-repeats and disease has motivated several investigations into the mechanism of aggregation and the role of Q-repeat length in aggregation. Curiously, glutamine repeats are common in vertebrates, whereas N-repeats are virtually absent in vertebrates, but common in invertebrates. One hypothesis for the lack of N-repeats in vertebrates is biophysical; that is, there is strong selective pressure in higher organisms against aggregation-prone proteins. If true, then asparagine and glutamine repeats must differ substantially in their aggregation properties despite their chemical similarities. In this work, aggregation of peptides with asparagine repeats of variable length (12−24) were characterized and compared to that of similar peptides with glutamine repeats. As with glutamine, aggregation of N-repeat peptides was strongly length-dependent. Replacement of glutamine with asparagine caused a subtle shift in the conformation of the monomer, which strongly affected the rate of aggregation. Specifically, N-repeat peptides adopted β-turn structural elements, leading to faster self-assembly into globular oligomers and much more rapid conversion into fibrillar aggregates, compared to Q-repeat peptides. These biophysical differences may account for the differing biological roles of N- versus Q-repeat domains.

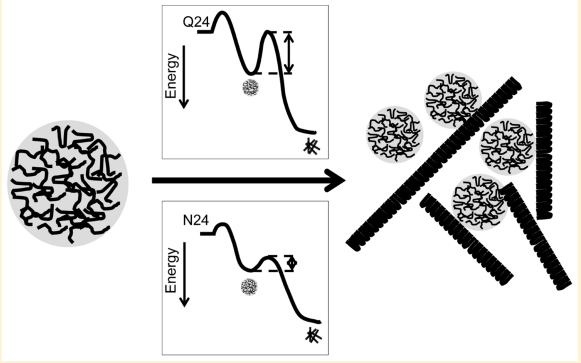

Amino acid repeat runs are common occurrences in eukaryotic proteins. In one survey of the human proteome, 20% of proteins were identified as containing one or more repeat tracts.[1] Of all repeat-containing (six or more identical amino acids in a run) eukaryotic proteins in the GENPEPT database, those containing glutamine (Q) are the most common.[2,3] Asparagine (N) repeats are the second most common in eukaryotes: curiously, these are abundant in invertebrates but rare or nonexistent in vertebrates.[1,2] For example, the human proteome contains 233 Q-repeats, but only eight N-repeats, all in a single protein. The opposite pattern occurs in the malarial parasite *Plasmodium falciparum*, where one-fourth of all proteins have N-repeats, but Q-repeats are nearly absent.[2] The amoeba *Dictyostelim discoideum* is extremely rich in both Q- and N-repeats,[4] and nearly 200 proteins in *Saccharomyces cerevisiae* have mixed Q/N-rich repeats.[5,6] This markedly nonrandom distribution of Q-repeats versus N-repeats in different eukaryotes is surprising, given the chemical similarity of glutamine and asparagine side chains.

Frequently, amino acid repeat domains lack a single stable structure, possibly because there are many energetically equivalent conformations.[7] In yeast, for example, proteins with abundant Q/N-rich repeats are depleted in hydrophobic and charged residues, further favoring population of a conformational ensemble rather than a unique defined structure.[6] In contradistinction to the conventional structure−function paradigm, the lack of a single stable folded structure is an important contributor to the function of repeat-containing proteins. In humans, glutamine repeats occur frequently in flexible disordered domains and are important in transcription regulation and the assembly of large macromolecular complexes, because their conformational adaptability allows for relatively promiscuous low-affinity interactions.[2,8] In Q/N-repeat yeast proteins, this structural adaptability provides an important mechanism for adaptive inheritance. Specifically, conversion from monomer to alternately folded fibril is triggered by environmental stresses. The structural conversion acts as a molecular switch to regulate translation, and, via the self-templating nature of the fibrillar aggregates, adaptation can be passed from mother to daughter cell.[9]

While some amino acid repeats (particularly hydrophobic) are constrained in length, glutamine and asparagine repeat run lengths are broadly distributed. Across the eukaryotic proteome, the repeat frequency decays with length; the vast majority are less than 20−25 residues, but there is a long tail in

Received: June 11, 2015
Revised: July 20, 2015
Published: July 23, 2015

DOI: 10.1021/acs.biochem.5b00644
Biochemistry 2015, 54, 4784−4794

the distribution, with some runs of 50 or more residues.[2] Trinucleotide repeats that encode for amino acid repeats are unstable, which in some cases leads to expansion of runs within a given protein and repeat-length polymorphism. Abnormal expansion of glutamine repeats is linked to at least nine progressive neurodegenerative disorders, including Huntington's Disease.[10] Proteins with expanded Q-repeats are prone to misfolding and/or aggregation, and it is hypothesized that the misfolding and aggregation lead to gain-of-toxic function that is intimately associated with disease mechanisms.[11] Ideally, the Q-repeat domain is long enough to carry out its regulatory and assembly functions, without being so long that it self-associates into toxic aggregates. Some invertebrates with a large number of repeat-rich proteins appear to have solved the aggregation problem by evolving unusually strong chaperone systems.[12,13] One hypothesis for the lack of N-repeats in vertebrates is biophysical, specifically, that there is strong selective pressure in most higher organisms against aggregation-prone proteins, because of their potentially toxic nature. If selection against aggregation-prone proteins is strong in vertebrates, then one would have to argue that N-repeats are substantially more aggregation-prone than Q-repeats, despite their chemical similarity. A few studies support this argument: yeast prion proteins with Q/N repeat domains that were relatively N-rich were more likely to form fibrillar, thioflavin-T positive, SDS-resistant aggregates compared to Q-rich repeat domains.[6,14] On the other hand, several groups have assumed, either directly or implicitly, that N- and Q-repeats are indistinguishable in their aggregation properties, e.g., refs 15−17.

Although synthetic Q-repeat peptides have proven to be a rich model system for investigating conformation and aggregation of Q-repeats (a few examples include refs 18−22), to our knowledge, there is no published work on aggregation kinetics of synthetic N-repeat peptides. In this investigation, we characterize the aggregation properties of N-repeat peptides of varying length and compare N-repeats with their Q-repeat "cousins". We tested whether the small chemical difference between asparagine and glutamine leads to any differences in the secondary structure or aggregation kinetics of N- and Q-repeats. Consideration must be given to the fact that "aggregates" is a very broad term that includes a diversity of noncovalently associated complexes ranging from soluble oligomers, to micron-size complexes of indeterminate morphology, to classic amyloid fibrils. The protein within these complexes could retain partial or complete native secondary structure, adopt an alternative fold, or populate an ensemble of irregular conformations. Therefore, we employed several complementary experimental tools in our investigation. We suggest that differences in the rate of aggregation as well as in the physical characteristics of the aggregates could provide a rationale for the marked frequency differences in the appearance of N- versus Q-repeats in proteins from different eukaryotic organisms.

MATERIALS AND METHODS

Peptide Synthesis and Purification. All materials were purchased from Fisher Scientific (Pittsburgh, PA) except where indicated. Peptides were synthesized using standard Fmoc solid-phase methods on a Protein Technologies Symphony synthesizer. Glutamine and asparagine with a trityl side chain protecting group, and lysine and tryptophan with Boc side chain protecting group, were purchased from Novabiochem (Gibbstown, NJ). The resin used was Fmoc-PAL-PEG-PS from Applied Biosystems (Foster City, CA). Half the resin sites were blocked with lysine-Boc to reduce on-bead aggregation. Extended and double couplings were used to improve yield. The peptide C-terminus was amidated and N-terminus acetylated. Peptides were cleaved from resin using 95% trifluoroacetic acid (TFA), 2.5% ethanedithiol (Fluka, Buchs, Switzerland), and 2.5% H_2O, precipitated into cold t-butylmethyl ether, and digested in water for 1 h before lyophilization.

Crude peptide was solubilized in a 1:1 solution of TFA and hexafluoroisopropanol (HFIP) with small amount of methionine added. The solution was evaporated under gentle N_2 flow, and the peptide was suspended in 55% TFA in water before purifying by reverse phase high performance liquid chromatography on a Vydac C18 column. Purified peptide was collected and confirmed by matrix-assisted laser desorption/ionization time-of-flight (MALDI-ToF) mass spectrometry.

Sample Preparation. Lyophilized purified peptides were disaggregated using our previously reported disaggregation protocol.[23] Briefly, peptides were dissolved in 20 μL of neat formic acid, vortexed, and centrifuged briefly 3 times within 1 min, then resuspended in pH 3 water. Peptide concentration was determined using tryptophan absorbance at 280 nm with an extinction coefficient of 5500 cm^{-1} M^{-1}. Samples were filtered, snap frozen, and stored at −80 °C. Prior to use, samples were thawed and filtered through 0.22 μm filter. All peptides were checked by native gel electrophoresis to ensure their monomer status.

Laser Light Scattering (LLS). All buffers were filtered through a 0.02 μm filter before use. Peptide samples were diluted into Tris buffer (200 mM, pH 8.4) to a peptide concentration of 30 μM and then immediately filtered through a 0.02 μm Whatman Anotop 10 (low-protein-binding) syringe filter (except where indicated) directly into a clean light-scattering cuvette and then placed into a bath of the index-matching solvent decahydronaphthalene held at 24 °C. In a few experiments as indicated, the samples were filtered through a 0.45 μm Millex low protein binding Durapore PVDF syringe filter instead of the Anotop. Light scattering data were collected at 90° scattering angle using a Brookhaven BI- 200SM system (Brookhaven Instruments Corp., Holtsville, NY) and an Innova 90C-5 argon laser (Coherent, Santa Clara, CA) operating at 488 nm and 150 mW. The z-averaged hydrodynamic diameter was determined from the autocorrelation function using the method of cumulants. Total scattered counts at the detector were collected for each sample. Scattered intensity of buffers was also measured; all buffer intensities were below 2 kcps (kilocounts per second) and subtracted from sample counts. For each measurement, data collection time was 5 min to ensure sufficient sampling.

Nanoparticle Tracking Analysis (NTA). Nanosight LM10 (Nanosight, Amesbury, UK) equipped with a 405 nm laser was used to collect NTA measurements. Samples were prepared as described above and were injected into the sample chamber using a syringe. Video capture was initiated immediately. For each experiment, one 30-s video was taken and analyzed using NTA 3.0 software. All measurements were collected at room temperature with camera level 13. All buffers were filtered through 0.02 μm filters before use and checked for absence of scattering particles, by observation of a completely blank background. Particle number concentration was calculated based on a scattering volume that is a function of instrument settings.

DOI: 10.1021/acs.biochem.5b00644
Biochemistry 2015, 54, 4784−4794

Circular Dichroism (CD). Peptide stock solutions were diluted into phosphate buffer (30 mM Na_2HPO_4/NaH_2PO_4 and 150 mM NaF, pH 7.4) to a peptide concentration of 25 μM. Freshly prepared samples were filtered through a 0.45 μm filter directly into a 1 mm cell. CD spectra were collected on an Aviv 202SF CD spectrophotometer from Aviv Biomedical (Lakewood, NJ) at 25 °C. Solvent spectra were collected and subtracted.

Thioflavin T (ThT) Fluorescence Assay. ThT stock solutions were prepared in Tris buffer and filtered through 0.22 μm filter. The concentration of ThT was measured using an extinction coefficient of 26 620 cm^{-1} M^{-1} at 416 nm, and the stock was diluted to a concentration of 73 μM. Peptide samples were diluted into Tris buffer to a concentration of 30 μM and filtered through a 0.02 μm filter immediately. After 1 h, 1 day, and 2 days of incubation at room temperature, 120 μL of sample was mixed with 20 μL of ThT stock. ThT fluorescence emission was measured using a QuantaMaster spectrofluorometer (PTI, Birmingham, NJ), with excitation at 440 nm and emission spectra recorded from 450 to 500 nm. Three replicates were collected and averaged. Fluorescence intensity at the peak (483 nm) was compared.

Luminescent Conjugated Oligothiophene (LCO) Fluorescence Assay. The LCO dye, h-FTAA, was generously donated by Dr. KPR Nilsson (Linkoping University, Sweden). h-FTAA stock solution was prepared by diluting the concentrated stock to 7.5 μM with Tris buffer. Peptide samples were diluted into Tris buffer to a concentration of 30 μM and filtered through a 0.02 μm filter immediately. Peptide samples were freshly prepared or incubated for 0.5 h, 1 h, 3 h, and 6 h at room temperature. After incubation, 110 μL of each sample was mixed with 15 μL of 7.5 μM h-FTAA, and incubated for 30 min. Fluorescence spectra were taken with excitation at 480 nm and emission spectra recorded from 500 to 680 nm. Three spectra were collected and averaged. Fluorescence intensity at the peak (553 nm) was compared.

SDS-PAGE Analysis. Peptide samples were diluted into Tris buffer to a concentration of 30 μM. Peptide samples diluted with pH 3 water to 30 μM were used as reference. After 1 h, 1 day, or 3 day incubation, samples were mixed with 16% sodium dodecyl sulfate (SDS) to a final SDS concentration of 2% and incubated for 1 h. Tricine sample buffer (2×) was added to peptide samples at a 1:1 ratio. Samples were loaded on a Novex (Life Technologies, Carlsbad, CA) 10−20% tricine gel, along with EZ-Run Protein Ladder (Fisher BioReagents, Fair Lawn, NJ), and electrophoresed using tricine SDS running buffer for 100 min at 125 V. Gels were silver stained (Pierce, Rockford, IL) following the manufacturer's protocol.

Filtration Assay. Peptides were diluted into Tris buffer to a concentration of 30 μM, incubated for 3, 6, 10, 14, and 17 days at room temperature. At each time point, 100 μL sample solution was taken and filtered through a 0.02 μm filter. The peptide concentration in the filtrate was measured by Nanodrop (Thermo Scientific, Wilmington, DE) using tryptophan absorbance at 280 nm with an extinction coefficient of 5500 cm^{-1} M^{-1}. All concentrations are reported as a percentage of the concentration of the initial unaggregated samples. The total absorbance at 280 nm increased slightly over time, most likely due to Trp oxidation,[23] so absorbances were corrected for this using Q12 or N12 as a reference.

Transmission Electron Microscopy (TEM). Peptides at 30 μM were prepared in Tris buffer and incubated for 4 h, 1 day, or 10 days at room temperature. A drop of sample was applied to a pioloform-coated grid and stained with methylamine tungstate stain. Images were taken with a Philips CM120 scanning transmission electron microscope (FEI Corp., Eindhoven, The Netherlands).

RESULTS

Peptide Synthesis, Purification, and Initial Characterization. Asparagine (N)-repeat peptides with the sequence $K_2WN_nAK_2$ were synthesized, where n = 12, 16, 20, or 24, using the synthesis protocol developed previously.[23] Flanking lysine residues were added to increase solubility, and tryptophan was used for concentration determination. Glutamine (Q)-repeat peptides with the same pattern ($K_2WQ_nAK_2$) were synthesized for comparison. After purification, peptides were disaggregated to achieve complete monomer as described previously.[23] Confirmation of identity and purity were obtained by mass spectrometry and gel electrophoresis (Figure S1). Measured molecular weights are 2198.2 (N12, 2198.3 theoretical), 2654.2 (N16, 2654.7 theoretical), 3110.5 (N20, 3111.1 theoretical), 3566.5 (N24, 3567.5 theoretical), 2366.3 (Q12, 2366.6 theoretical), 2878.5 (Q16, 2879.1 theoretical), 3390.7 (Q20, 3391.7 theoretical), and 3903.7 (Q24, 3904.2 theoretical).

Several algorithms have been developed to predict aggregation-prone regions in proteins, and we wondered if these would reveal any aggregation propensity for, or any differences between, N- and Q-repeat peptides. We analyzed the sequences of N24 and Q24 using four different algorithms: Aggrescan,[24] FoldAmyloid,[25] TANGO[26,27] and Zyggregator.[28] No aggregation-prone regions were identified in any of the algorithms for either N24 or Q24. TANGO predicted one distinction: that N24 has strong β-turn propensity whereas Q24 has none, and Q24 has moderate β-sheet propensity versus almost none for N24 (Figure S2).

Previously we reported CD spectra of N24 and Q24.[23] Compared to Q24, N24 spectra showed a blueshift in the position of the minimum (from 201 to 197 nm), a decrease in (absolute) value of ellipticity at the minimum, and a flattening of the shoulder from 212 to 225 nm. In this study, we collected additional CD spectra for freshly prepared solutions of N12, N16, N20, Q12, Q16, and Q20. Spectra of N-repeat peptides were all virtually identical, indicating that secondary structure is not length-dependent (Figure 1). Spectra of Q-repeat peptides

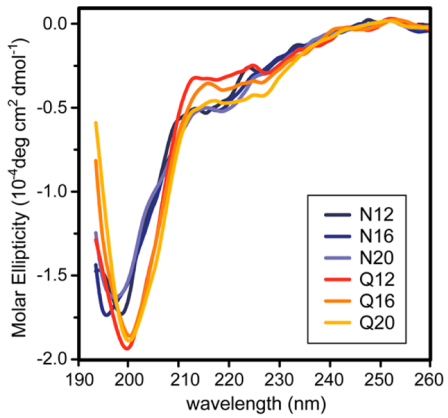

Figure 1. CD spectra of N-repeat and Q-repeat peptides. Peptide stock solutions were diluted into phosphate/NaF buffer (30 mM Na_2HPO_4/NaH_2PO_4 and 150 mM NaF, pH 7.4) to a peptide concentration of 25 μM. Solvent spectra were collected and subtracted.

DOI: 10.1021/acs.biochem.5b00644
Biochemistry 2015, 54, 4784−4794

were also length-independent except for a small shift around 210−230 nm. N-repeat and Q-repeat peptides differed from each other as observed previously for N24 and Q24. Most notable is the shift in the position and depth of the minimum. Such shifts in CD spectra are attributed to a partial shift from disordered to β-turn for N24,[29,30] consistent with the TANGO prediction (Figure S2). Also consistent with these data, molecular dynamics simulations show that N-repeat peptides, although predominantly disordered, have some β-turn content[31] and that N-repeats can form tighter β-turns than Q-repeats because of asparagine's shorter side chain.[14]

Influence of Sample Preparation Method on Aggregation of N24 and Q24. We chose N24 and Q24 for an initial evaluation of aggregation, using laser light scattering (LLS) and nanoparticle tracking analysis (NTA). With both techniques, measurements are in-solution and noninvasive, and require no labeling. Light scattering techniques are most suitable for measuring the hydrodynamic size (and change in size) of soluble, freely diffusing submicron particles. For LLS experiments, two types of data are collected: the total scattered intensity at 90° scattering angle (an approximate indicator of the relative number and molecular weight of all particles in solution) and the mean apparent hydrodynamic diameter (by analysis of the mean fluctuations in scattered intensity due to diffusive motion). Nanoparticle tracking analysis (NTA) is a scattering technique to visualize and measure the diffusive motion of nanoparticles in solution. Particles in solution scatter light from an incident laser, and the scattered light signal is recorded by a high sensitivity CCD camera. NTA is a particle-by-particle method; therefore, the size distribution and the number concentration can be obtained simultaneously. Compared to intensity-averaged methods like LLS, NTA has less bias toward larger particles. NTA is extremely sensitive to the presence of even a very low number of particles, but has a size limit of detection of >30 nm for proteins.[32,33] The technique is also limited to a relatively narrow range of particle number concentration and relatively slow kinetics of growth; additionally, caution must be exercised in analyzing aggregates with a very large aspect ratio.[32,33]

We prepared monomeric stocks of N24 and Q24, then diluted into Tris buffer (200 mM, pH 8.4) to initiate aggregation. The samples were immediately filtered through one of two different pore size filters: 0.02 or 0.45 μm. Concentrations were checked before and after filtration; there was no measurable change in concentration with either filter. Samples were then evaluated by LLS. With N24 filtered through 0.45 μm filters, aggregates were observed after a short (~2 min) delay time. The count rate grew rapidly (Figure 2a) as did the particle hydrodynamic diameter, reaching an apparent mean size of ~4000 nm at 1.5 h (not shown). With Q24 filtered through 0.45 μm filter, aggregates were detected approximately 30 min after sample preparation (Figure 2a). The rate of increase in scattered intensity was much slower for Q24 than for N24; still, the particles reached a large hydrodynamic diameter of ~2300 nm at 1 h (not shown). With filtration through the tighter pore-size (0.02 μm) filter, N24 aggregation was negligibly affected except for a slight increase in the lag time (Figure 2b). In contrast, Q24 aggregation was completely suppressed by the tighter filter over the 90 min monitoring time.

To further investigate, Q24 samples were examined by NTA immediately after dilution and filtration. For the sample filtered through the 0.45 μm filter, during the 30 min window where no

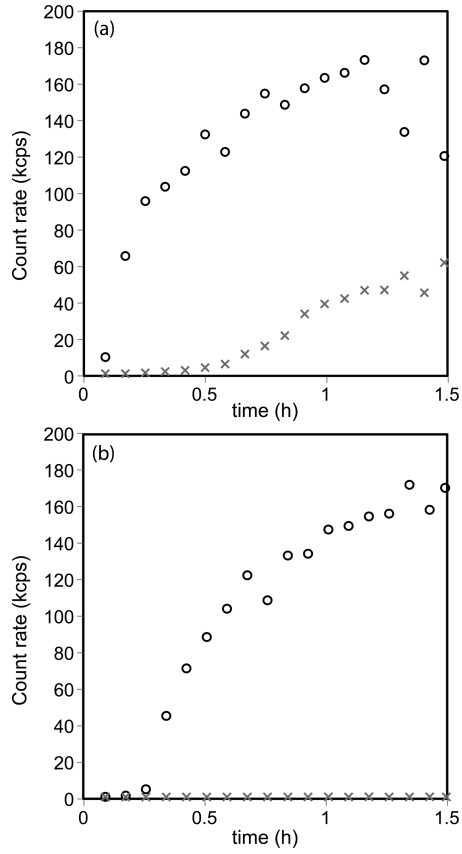

Figure 2. Comparison of aggregation kinetics as measured by scattering counts for N24 (○) and Q24 (×). Peptides were prepared at 30 μM in Tris buffer from monomeric stocks. Aggregation kinetics were observed after (a) filtration through 0.45 μm filter and (b) filtration through 0.02 μm filter.

aggregates were detected by LLS, by NTA we observed a few particles of ~60 nm diameter. Over 60 min, the number concentration increased from 1.4×10^6 to 4×10^8 particles/mL (2 fM to 0.7 pM). These data demonstrate the high sensitivity of NTA to the presence of aggregates at extremely low particle concentrations. This low level of aggregates would never be detectable by mass-balance-based methods such as absorbance or HPLC. Moreover, these results indicate that dilution and/or mixing induces a small degree of aggregation, possibly due to transient gradients in concentration and/or pH. No aggregates were detected by NTA if the Q24 sample was filtered through a 0.02 μm filter postdilution, over a 60 min observation time. The distinctly different outcomes of removing these aggregates in Q24 versus N24 demonstrate that under quiescent conditions, N24 forms new aggregates much more quickly than does Q24. Since the growth rate of N24 aggregates is independent of the presence of any pre-existing aggregates, we suggest that in the early stages of N24 self-association, a pseudoequilibrium state is rapidly reached. On the other hand, with Q24 there is a strong influence of the condition of the starting solution, demonstrating that the initial self-association of Q24 under quiescent conditions is very slow and under kinetic control. On the basis of these data, all remaining experiments were conducted with 0.02 μm filtration postdilution.

Length-Dependent Aggregation Kinetics of N-Repeat Peptides. With Q-repeat peptides, typically, a repeat length of 20 glutamines or more is required to observe aggregation, depending on flanking residues, buffer conditions, and peptide

DOI: 10.1021/acs.biochem.5b00644
Biochemistry 2015, 54, 4784−4794

concentration. It is also well established that the rate of aggregation increases rapidly with an increase in Q-repeat length.[18,20,34−36] To our knowledge, length-dependence of aggregation of N-repeat peptides has not been previously investigated.

We used LLS and NTA to characterize the aggregation kinetics of peptides containing repeats of 12− 24 asparagines. Briefly, peptides were diluted from stock (monomeric) solutions into Tris buffer to a final concentration of 30 μM, to induce aggregation. Immediately after dilution, samples were filtered through a 0.02 μm filter to remove any aggregates formed during the dilution process. Concentrations were checked before and after filtration and were unchanged. LLS data were collected for 90 min; both total scattered intensity and hydrodynamic diameter were measured. For N12 and N16, no evidence of aggregation was detected over the time course of the experiment (Figure 3). For N20, there were no

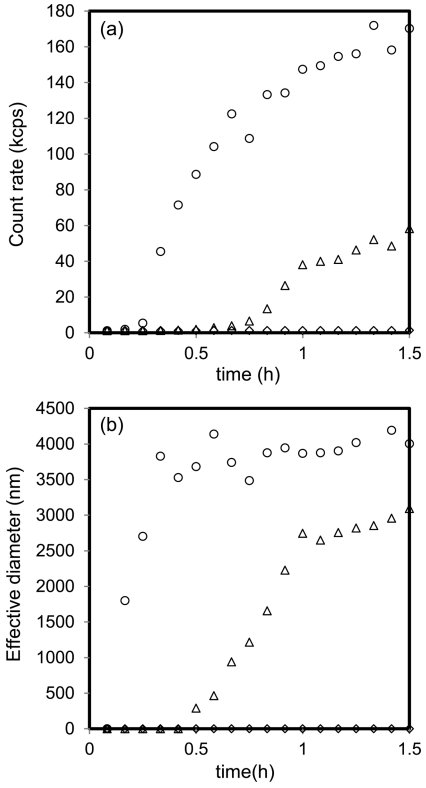

Figure 3. Laser light scattering analysis of aggregation of N-repeat peptides as a function of N-repeat length. Peptides were prepared at 30 μM in Tris buffer from monomeric stocks. (a) Total scattered counts detected at 90° scattering angle, with buffer subtracted. (b) Mean apparent hydrodynamic diameter determined by cumulants analysis of autocorrelation functions. N16 (◊), N20 (Δ), or N24 (○).

aggregates detected in the first 30 min, at which point aggregates started to form and then increased in size to ∼3000 nm. For N24, aggregates were detected less than 5 min after sample preparation. The effective diameter increased rapidly and reached ∼4000 nm in less than 30 min. The scattered intensity at 90 min was about 3-fold higher for N24 than for N20.

Similarly prepared samples were analyzed by NTA. Samples were repeatedly observed for 1 h postdilution, with a 30-s time window for each observation. For N12 and N16, we did not observe any scattering particles, consistent with the LLS results. For N20, almost no particles (one or none) were observed up to 35 min, a lag time consistent with the data in Figure 3. At 35 min, weakly scattering, rapidly diffusing particles started to appear; these grew in both size and number concentration over the next half hour (Figure 4a, Figure S3a). With N24, a few

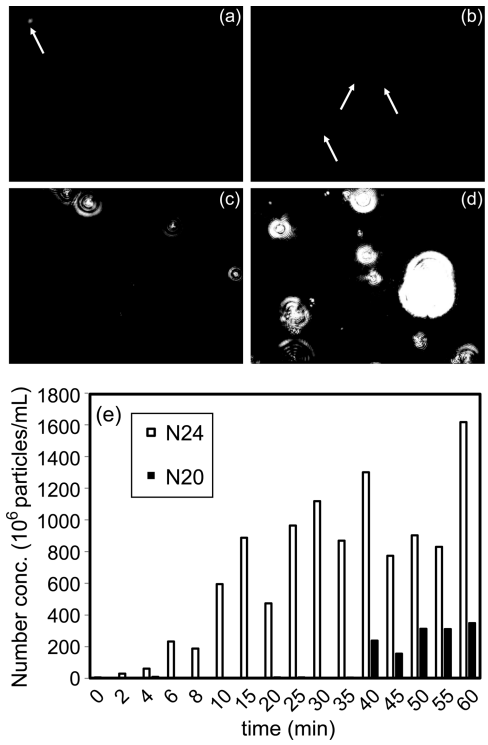

Figure 4. NTA analysis of aggregation of N-repeat peptides as a function of N-repeat length. Peptides were prepared at 30 μM in Tris buffer from monomeric stocks. (a−d) Still images taken from videos collected for (a) N20 at 35 min, (b) N24 at 2 min, (c) N20 at 40 min, and (d) N24 at 40 min. (e) Particle number concentration as a function of time for N20 or N24. 10^9 particles/mL is equivalent to 1.6 pM.

small particles appeared at 2 min (Figure 4b, Figure S3b), and the particle number concentration increased steadily over the next 15 min. At approximately 10−15 min, we observed the clustering together of scattering centers, presumably due to coalescence of smaller aggregates. After 25 min, very large, strongly scattering aggregates appeared suddenly; the diffraction rings attest to the micron (or greater) size of the aggregates. A comparison of N20 and N24 at 40 min is shown in Figure 4c,d, and Figure S3c,d. Aggregates were much more numerous in N24 than in N20 (Figure 4e). The mean size of N20 aggregates increased from 73 nm (35 min) to 360 nm (50 min). (Note that NTA analysis yields a number-average diameter versus the intensity-averaged diameter from dynamic light scattering. The difference in mean diameter is attributable to a very broad particle size distribution.) N24 aggregates grew too fast and scattered too strongly to conduct a meaningful analysis of particle size distribution.

Structural Characterization of N24 and Q24 Aggregates Based on Dye-Binding and SDS Solubility. We next used two different fluorescence dyes, h-FTAA and ThT, to detect formation of prefibrillar or fibrillar aggregates. h-FTAA is one of a class of luminescent conjugated oligothiophenes (LCO) that fluoresce when bound to prefibrillar protein

DOI: 10.1021/acs.biochem.5b00644
Biochemistry 2015, 54, 4784−4794

aggregates.[37] Thioflavin T (ThT), one of the most commonly used fluorophores for detecting amyloid fibrils, is believed to bind to the long axis of the fibrils, requiring a ladder of 4−5 cross-β strands.[38] LCO and ThT dyes are believed to bind to similar cross-β-sheet structural features, but LCO dyes also detect shorter fibrils or prefibrillar aggregates that are ThT-negative. For example, beta-amyloid aggregates are detectable with LCO prior to their conversion to ThT-positive aggregates.[39] With both dyes, binding to aggregates is detected by a large increase in fluorescence intensity, and intensity is considered to be proportional to the mass concentration of prefibrillar or fibrillar aggregates.

Immediately after sample preparation, neither N24 nor Q24 induced any h-FTAA fluorescence above background (Figure 5a). N24 developed strong h-FTAA signal intensity by 0.5 h

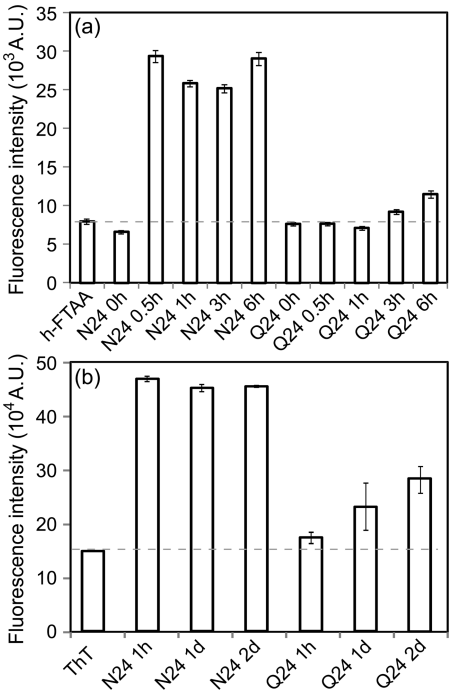

Figure 5. Kinetics of fibrillogenesis of N24 and Q24, as measured by (a) h-FTAA and (b) ThT. Samples were incubated for 0 h, 0.5 h, 1 h, 3 h, and 6 h for h-FTAA assay and 1 h, 1 day, and 2 days for ThT assay. The dashed line indicates background fluorescence intensity in the absence of added peptide.

that remained constant over 6 h. In contrast, there was no fluorescence above background in the Q24 sample for the first 3 h, after which there was a slow increase in fluorescence. At 6 h, the signal intensity for Q24 was only about one-fifth that of N24. ThT results were taken over a longer time period but were qualitatively similar: we observed strong fluorescence at the first measurement time (1 h) for N24, and the fluorescence signal remained constant for 2 days (Figure 5b). In contrast, Q24 was ThT-negative at 1 h; fluorescence increased slowly over the next 2 days but was still only half the fluorescence as N24 after just 1 h.

We next compared Q24 and N24 for resistance to dissociation in SDS, a test that has been used to distinguish amyloid fibrils from nonamyloid protein complexes.[40,41] Samples (30 μM) were incubated for 1 h, 1 day, or 3 days, then adjusted to 2 (w/w)% SDS for 1 h, before analysis by gel electrophoresis. Under these conditions, SDS-susceptible aggregates dissociate into monomers, while SDS-resistant aggregates do not enter the tricine gel. With Q24, the intensity of monomer bands did not change compared to the unaggregated sample after 1 h or 1 day, indicating that essentially all material remained SDS-soluble during this time. After 3 days there was a slight decrease in monomer band, indicating the formation of some SDS-insoluble species (Figure 6a). For N24, monomer band intensity dropped slightly after 1

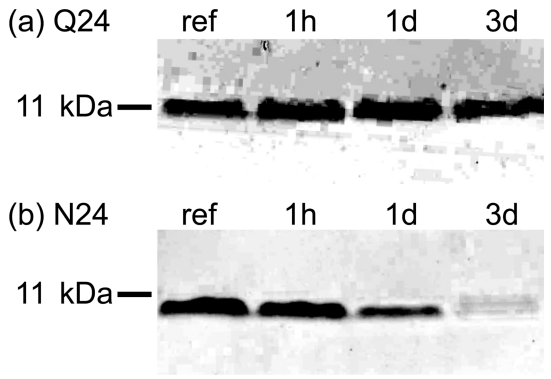

Figure 6. Development of SDS-insoluble aggregates. (a) Q24 and (b) N24 samples (30 μM) were incubated for 1 h, 1 day, or 3 days, adjusted to 2 (w/w)% SDS for 1 h, then analyzed by gel electrophoresis. Samples diluted with pH 3 water to the same concentration were measured as reference.

h and measurably after 1 d, indicating SDS-resistant aggregates developed during the aggregation process. By 3 days, much of the peptide was in SDS-resistant aggregates (Figure 6b).

Taken together, the data in Figures 3−6 are all consistent with a similar picture. Briefly, under these experimental conditions, N24 rapidly (<5 min) forms soluble aggregates that undergo a transition to large, fibrillar aggregates within 0.5−1 h. Further maturation to SDS-resistant amyloid aggregates occurs subsequently over the course of a few hours to a few days. Q24, in contrast, requires several (~2) hours before aggregates are detected even by sensitive techniques, and those aggregates grow only slowly into prefibrillar and fibrillar aggregates, which require several days to develop into SDS-insoluble aggregates.

Kinetics of Incorporation into Aggregates, and Morphology of Aggregates. A filtration assay was used to study kinetics over a longer time course. Briefly, samples were incubated for up to 17 days. Aliquots were taken at regular intervals and filtered through a 0.02 μm filter, and the peptide concentration in the filtrate was measured. This experiment measures the mass fraction of peptide that is incorporated into stable particles larger than ~20 nm (e.g., retained by a 20 nm cutoff capillary pore filter). N16, N20, and N24 all formed some aggregates that were removed by nanofiltration (Figure 7). Peptide concentration in the filtrate reached a steady state by the time of the first measurement (3 days), with approximately 15% of N16, 25% of N20, and 40% of N24 removed by nanofiltration. Compared to the data in Figure 2, these results suggest that the length of the N-repeat has a greater effect on the rate of increase of aggregate size and a lesser (though still substantial) effect on the steady-state mass fraction of peptide incorporated into aggregates. It should be pointed out that, although the mass fraction of aggregated peptide reaches steady state, these data cannot address the

DOI: 10.1021/acs.biochem.5b00644
Biochemistry 2015, 54, 4784−4794

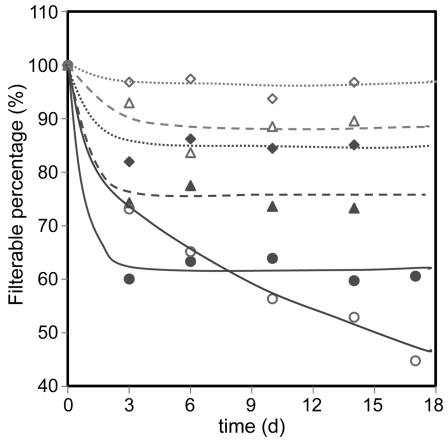

Figure 7. Kinetics of loss of peptide from solution. Peptides [Q24 (○), Q20 (Δ), Q16 (◊), N24 (●), N20 (▲), and N16 (♦)] were diluted to 30 μM and incubated at room temperature. At the time indicated, 100 μL sample was taken and filtered through 0.02 μm filter and the concentration of filtrate was measured by Nanodrop. The percentage reported is compared to the concentration at time zero.

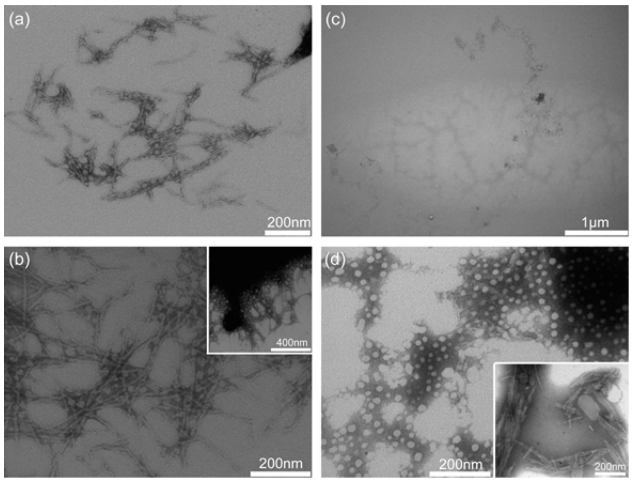

Figure 8. TEM images. Samples were at 30 μM and incubated at room temperature. (a) N24 at 4 h incubation. (b) N24 at 1 day incubation. Inset: 400 nm scale (c) Q24 at 4 h incubation. (d) Q24 at 1 day incubation. Inset: Q24 at 10 day incubation.

question as to whether peptide conformation, or aggregate size or morphology, is also equilibrated.

Much less of Q16 and Q20 was removed by nanofiltration compared to N16 and N20, with only ~2% and ~10% peptide loss, respectively. With Q24, the amount of peptide removed by nanofiltration increased slowly and steadily over the 17-day period (Figure 7). The retained fraction was less for Q24 than N24 at 3 days, became equal at 8 days, and was greater (55%) after 17 days. These data on Q16, Q20, and Q24 are reasonably consistent with previously reported experiments taken under slightly different conditions, where aggregate mass fraction was measured by sedimentation rather than filtration.[20] Thus, the rate of self-association of Q24 is slower, but a larger fraction of Q24 eventually self-associates, compared to N24. It is interesting to note that at 3 days, both N24 and Q24 contain a substantial fraction of filterable aggregates (Figure 7), but Q24 aggregates are still mostly SDS-soluble whereas N24 aggregates are mostly not (Figure 6). This suggests a much slower rate of conversion of Q24 nonfibrillar and prefibrillar aggregates into mature (SDS-insoluble) fibrils.

Finally, we examined N24 and Q24 by transmission electron microscopy (TEM). With N24, after 4 h, a mix of fibrils and globular protein clusters were observed (Figure 8a). After 1 day, N24 contained numerous well-defined thin fibrils, as well as some globular clusters (~30 nm diameter) and a few very large inclusions (Figure 8b and inset). In contrast, we saw virtually no aggregates in Q24 incubated for 4 h (Figure 8c). After 1 d incubation, we observed predominantly globular protein clusters with diameters of approximately 30−50 nm but very few fibrils (Figure 8d). Given the much slower aggregation kinetics for Q24 compared to N24, we examined Q24 by TEM after incubation for 10 days. There was a striking change in morphology to large sheet-like bundles of fibrils (Figure 8d inset). These fibrils were identical in morphology to those observed previously for a similar Q-repeat peptide.[29]

DISCUSSION

Interest in aggregation of Q-repeat domains is motivated by the involvement of expanded glutamine domains in a number of neurodegenerative diseases including Huntington's.[10,11] For this reason, there have been numerous investigations of aggregation of peptides and proteins containing Q-repeat domains (e.g., refs 19, 20, and 22). N-repeats have received very little attention, presumably because of their nearly complete absence in the human proteome and, indeed, in all vertebrates. However, N-repeats are quite common in non-vertebrate eukaryotes,[1,2] a curious finding given the chemical similarity between glutamine and asparagine.[2] The two amino acids both have amide side chains, which participate in hydrogen bonds as both donor and acceptor, and differ only by a single additional methylene group in glutamine. Asparagine is slightly more hydrophilic than glutamine.[42] Glutamine's longer side chain confers additional conformational entropy, while asparagine's smaller side chain more easily accommodates tight β-turns.[14] By evaluating aggregation in N-repeat peptides, and by comparing Q- versus N-repeats, we hoped to determine to what extent the small difference in side chain gave rise to different aggregation phenomena. Results from such investigations could then inform theories as to the distinct evolutionary pathways followed by different eukaryotes, where N-repeats are variously suppressed or allowed.

We used several biophysical tools to characterize and compare the aggregation kinetics of N24 and Q24. A comparison is summarized in Table 1. Taken together, the data are consistent with the following pathway. Monomeric N24 rapidly self-associates into globular aggregates of roughly 30−50 nm diameter. Around 30 min after initiation of aggregation, the concentration of globules has increased sufficiently that there is a fast transition, visualized by NTA, as the globules coalesce into very large aggregates. These aggregates are LCO-positive, ThT-positive, and SDS-soluble, indicating that they have adopted fibrillar structures but are not yet fully mature fibrils. After 1 day, the aggregates have become increasingly resistant to SDS, indicating a conversion to mature, compact fibrils. Q24 aggregation was markedly slower than N24 in all phases. Under the experimental conditions used in this study, no aggregates were detected over the first 90 min even by sensitive light scattering techniques. LCO-positive/ThT-positive aggregates appeared only after several hours, and the increase in fluorescence was slow and measured rather than rapid, in contrast to N24. The predominantly globular aggregates, observed in TEM images after 1 day, are

DOI: 10.1021/acs.biochem.5b00644
Biochemistry 2015, 54, 4784−4794

Table 1. Comparison of Aggregation Characteristics of N24 versus Q24

technique	DLS	h-FTAA	ThT	SDS	TEM
measured property	time to appearance of soluble aggregates	time to appearance of prefibrillar aggregates	time to appearance of fibrillar aggregates	solubility in SDS at 3 days	aggregate morphology
N24	~ 0.05 h	< 0.5 h	< 1 h	mostly insoluble	thin fibrils and large inclusion body
Q24	~ 2 h	> 6 h	> 24 h	mostly soluble	sheet-like bundles of fibrils

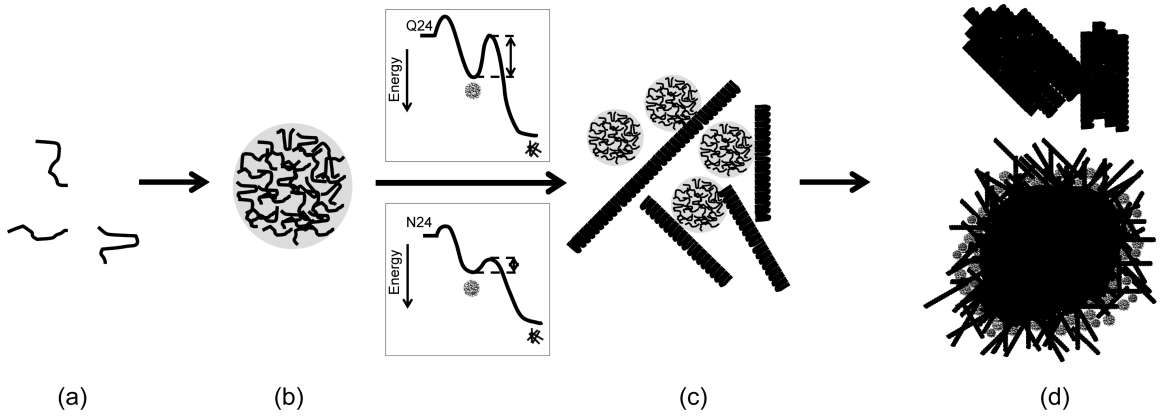

Figure 9. Schematic illustrating growth of N24 and Q24 particles. Initially present as monomers (a), both peptides self-assemble into soluble globular clusters of ~30 nm (N24) to ~50 nm (Q24) (b). Globular clusters coalesce into larger aggregates and undergo conformational rearrangement to fibrillar aggregates (c). Fibrils mature further and associate into large inclusions (N24) or sheets (Q24) (d).

morphologically similar to, but somewhat larger than, the globules of N24 that appeared within hours. Q24 aggregates remained SDS-soluble for several days. Thus, Q24 aggregates remain in intermediate states, as globules and/or immature fibrils, for much longer than N24.

Although glutamine monomers or short glutamine domains are highly solvated with water,[21,43] repeat domains containing 15 or more glutamines are compact and collapsed, due to formation of intramolecular hydrogen bonds (involving both backbone and side chain).[20,44,45] These compact structures do not contain any regular secondary structure such as β-sheet and are remarkably stable; it has been estimated that at least 17 hydrogen bonds must be broken before the polypeptide chain can be extended.[45] We and others have previously proposed that these compact monomers are poorly solvated with water and coalesce into soluble oligomers; subsequent structural rearrangement within the "liquid-like" oligomer produces ordered aggregates with β-sheet hydrogen bonding patterns and fibrillar morphologies.[20,46,47] This mechanism is sometimes called the "association-conformational conversion" model of polyglutamine aggregation. Conversion from the disordered oligomer to the regular fibrillar structure requires breaking and making hydrogen bonds, packing of backbones and side chains into a regular array, and exclusion of water. We propose that the association-conformational conversion model also applies to N24, but with distinct kinetic features. Specifically, the kinetic barrier for conversion from soluble globular oligomers to LCO/ThT-positive fibrils, as well as the maturation to SDS-resistant fibrils, is decidedly lower for N24 compared to Q24 (Figure 9). Over several days, a greater fraction of Q24 is converted into aggregates compared to N24, suggesting that the thermodynamic driving force for conversion of monomers to aggregates is greater for Q24 than for N24, (keeping in mind that this analysis is oversimplified as the aggregate population is heterogeneous). Greater mechanistic insight and testing of this hypothesis could be obtained through close examination of the concentration-dependent behavior.

One explanation for the faster kinetics of N24 compared to Q24 is the former's tendency to adopt β-turns (Figure 1). This conclusion is supported by previous studies of a Q-repeat peptide in which two central residues were replaced with the β-turn template ^{D}Pro-Gly.[29] The CD spectra of N24 closely resembled the spectra obtained in that previous study, and the imposition of the β-turn template in the Q-repeat peptide dramatically accelerated the rate of formation of sedimentable aggregates,[29] much as we observed here by replacing Q with N. Such a template helps to align side chains for adoption of β-sheet fibrillar structure. Additionally, the longer glutamine side chain has greater conformational entropy than asparagine, and must sample more conformational space, in order to achieve regular alignment within β-sheets. Once aligned, though, the greater contact between the longer hydrophobic alkyl chain of glutamine should be energetically more favorable, providing one possible explanation as to why a greater mass fraction of Q24 is aggregated at long time, even though the rate at which it aggregates is much slower than N24. For both Q- and N-repeat peptides, the secondary structure has little or no length dependence, but aggregation rates are strongly length dependent, with a minimum length around 16 residues for asparagine and 20 residues for glutamine under our experimental conditions (Figure 7). Thus, the tendency to adopt β-turns distinguishes N-repeats from Q-repeats and greatly accelerates the *rate* of aggregation. The tighter β-turn adopted by asparagine compared to glutamine[14] may account for the slightly longer run length required in Q-repeats for *existence* of aggregates.

Important morphological differences are evident over longer periods of time as well. A network of fibrils, very large agglomerates of fibrils, and some small globules are evident in TEM images of N24 taken after 1 day. Q24, in contrast,

DOI: 10.1021/acs.biochem.5b00644
Biochemistry 2015, 54, 4784−4794

associates into bundled sheets and ribbons of fibrils. The long thin fibrils of N24 are morphologically very similar to those observed previously with the Q-repeat peptide with the β-turn template.[29] The β-turn prevented lateral alignment into bundled sheets and ribbons,[29] and supported elongation of a more compact and dehydrated fibril.[48] These results suggest that there may be structural distinctions within the fibrils that influence fibril−fibril interactions.

Whether these biophysical differences between Q-repeats and N-repeats can explain the differences in frequency of repeats in vertebrates compared to invertebrates remains an open question. Our experimental data provide some basis for conjecture. The lack of regular structure in Q-repeat domains likely facilitates the functioning of these proteins as 'assemblers, chaperones, and scavengers':[49] affording their participation in formation of multiprotein complexes, signal transduction, and regulation of transcription.[50−52] One of the key functions of Q-repeat domains is to mediate and stabilize protein−protein interactions, and a longer Q-repeat domain leads to greater interaction capacity.[53] However, a longer Q-repeat also confers a greater risk of aggregation, a process that may normally be kept under control through chaperones and other components of the proteostasis machinery.[54] In this regard, Q-repeat runs are conspicuously absent in prokaryotes; it has been speculated that such organisms lack a sufficiently strong clearance mechanism for targeting and degrading aggregated proteins.[53] On the other side of the coin, eukaryotic invertebrates (*P. falciparum* and *D. discoideum*) with an unusually large fraction of proteins with N- or Q/N-repeats have evolved a very robust system for chaperoning proteins and limiting aggregation.[12,13]

On the basis of our data, we hypothesize the existence of a higher kinetic energy barrier between monomer and oligomer, and between amorphous globular and fibrillar aggregates, for Q24 than for N24. Thus, Q24 is slower to aggregate, and its aggregates remain in intermediate states as soluble globules and/or nonfibrillar/prefibrillar aggregates for much longer, than N24. There is substantial evidence that in expanded-glutamine disorders such as Huntington's, soluble, less-ordered aggregates are more toxic than fully mature fibrils.[55−57] Since these diseases are late-onset, the inability to adequately degrade Q-repeat aggregates may arise from age-related failure of the protein quality control machinery, and would not be under strong evolutionary pressure. Thus, the slower kinetics of aggregation for Q-repeats may be advantageous in maintaining them more stable in their functional state compared to N-repeats, but at the price of the potential for greater exposure to toxic aggregates.

Much less is known about the function of N-repeats in monomeric proteins, but the role of N-repeats (or mixed Q/N repeats) in conversion of yeast prion proteins from monomer to fibril has been well-studied. These organisms take advantage of the greater self-assembly and fibrillogenic propensity of N-repeats as a means of adaptive inheritance in response to environmental stress.[58] Since prefibrillar aggregates cannot serve as reliable templates, rapid conversion from monomer to fibril is important for the adaptive inheritance function of prions, and thus N-rich repeats may be selected for in those organisms where faithful prion templating provides a survival advantage. The function and aggregation properties of repeat domains of these two ostensibly similar amino acids have diverged biologically, and a comparison of the biophysical properties of synthetic peptides may help to illuminate the reasons why.

■ ASSOCIATED CONTENT

Supporting Information

The Supporting Information is available free of charge on the ACS Publications website at DOI: 10.1021/acs.biochem.5b00644.

Figure S1: Mass spectra of synthesized and HPLC-purified peptides and Native gel electrophoresis post formic acid disaggregation; Figure S2: Analysis of N24 and Q24 by TANGO (PDF)
Figure S3: (a) NTA video, N20, 35 min, Video 1 (MPG)
(b) NTA video, N24, 2 min, Video 2 (MPG)
(c) NTA video, N20, 40 min, Video 3 (MPG)
(d) NTA video, N24, 40 min, Video 4 (MPG)

■ AUTHOR INFORMATION

Corresponding Author

*Address: 1415 Engineering Dr., Madison, WI 53706. E-mail: regina.murphy@wisc.edu.

Funding

Funding was provided by the National Science Foundation CBET-1262729.

Notes

The authors declare no competing financial interest.

■ ACKNOWLEDGMENTS

CD spectra were obtained at the University of Wisconsin-Madison Biophysics Instrumentation Facility, which was established with support from the University of Wisconsin-Madison and grants BIR-9512577 (NSF) and S10 RR13790 (NIH), with technical assistance provided by Dr. Darrell McCaslin. Peptides were synthesized at the University of Wisconsin-Madison Biotechnology Center with technical assistance provided by Nina Porcaro. Dr. K. Peter Nilsson of Linkoping University kindly provided the h-FTAA dye.

■ ABBREVIATIONS

CD, circular dichroism; h-FTAA, heptameric formic thiophene acetic acid; LCO, luminescent conjugated oligothiophene; LLS, laser light scattering; NTA, nanoparticle tracking analysis; SDS-PAGE, sodium dodecyl sulfate−polyacrylamide gel electrophoresis; TEM, transmission electron microscopy; ThT, thioflavin T

■ REFERENCES

(1) Karlin, S., Brocchieri, L., Bergman, A., Mrazek, J., and Gentles, A. J. (2002) Amino acid runs in eukaryotic proteomes and disease associations. *Proc. Natl. Acad. Sci. U. S. A. 99*, 333−338.

(2) Faux, N. G., Bottomley, S. P., Lesk, A. M., Irving, J. A., Morrison, J. R., de la Banda, M. C., and Whisstock, J. C. (2005) Functional insights from the distribution and role of homopeptide repeat-containing proteins. *Genome Res. 15*, 537−551.

(3) Faux, N. G., Huttley, G. A., Mahmood, K., Webb, G. I., Garcia de la Banda, M., and Whisstock, J. C. (2007) RCPdb: An evolutionary classification and codon usage database for repeat-containing proteins. *Genome Res. 17*, 1118−1127.

(4) Eichinger, L., Pachebat, J. A., Glockner, G., Rajandream, M. A., Sucgang, R., Berriman, M., Song, J., Olsen, R., Szafranski, K., Xu, Q., Tunggal, B., Kummerfeld, S., Madera, M., Konfortov, B. A., Rivero, F., Bankier, A. T., Lehmann, R., Hamlin, N., Davies, R., Gaudet, P., Fey, P., Pilcher, K., Chen, G., Saunders, D., Sodergren, E., Davis, P., Kerhornou, A., Nie, X., Hall, N., Anjard, C., Hemphill, L., Bason, N., Farbrother, P., Desany, B., Just, E., Morio, T., Rost, R., Churcher, C., Cooper, J., Haydock, S., van Driessche, N., Cronin, A., Goodhead, I.,

DOI: 10.1021/acs.biochem.5b00644
Biochemistry 2015, 54, 4784−4794

Muzny, D., Mourier, T., Pain, A., Lu, M., Harper, D., Lindsay, R., Hauser, H., James, K., Quiles, M., Madan Babu, M., Saito, T., Buchrieser, C., Wardroper, A., Felder, M., Thangavelu, M., Johnson, D., Knights, A., Loulseged, H., Mungall, K., Oliver, K., Price, C., Quail, M. A., Urushihara, H., Hernandez, J., Rabbinowitsch, E., Steffen, D., Sanders, M., Ma, J., Kohara, Y., Sharp, S., Simmonds, M., Spiegler, S., Tivey, A., Sugano, S., White, B., Walker, D., Woodward, J., Winckler, T., Tanaka, Y., Shaulsky, G., Schleicher, M., Weinstock, G., Rosenthal, A., Cox, E. C., Chisholm, R. L., Gibbs, R., Loomis, W. F., Platzer, M., Kay, R. R., Williams, J., Dear, P. H., Noegel, A. A., Barrell, B., and Kuspa, A. (2005) The genome of the social amoeba Dictyostelium discoideum. *Nature 435*, 43−57.

(5) Michelitsch, M. D., and Weissman, J. S. (2000) A census of glutamine/asparagine-rich regions: Implications for their conserved function and the prediction of novel prions. *Proc. Natl. Acad. Sci. U. S. A. 97*, 11910−11915.

(6) Alberti, S., Halfmann, R., King, O., Kapila, A., and Lindquist, S. (2009) A systematic survey identifies prions and illuminates sequence features of prionogenic proteins. *Cell 137*, 146−158.

(7) Tran, H. T., Mao, A., and Pappu, R. V. (2008) Role of backbone - Solvent interactions in determining conformational equilibria of intrinsically disordered proteins. *J. Am. Chem. Soc. 130*, 7380−7392.

(8) Atanesyan, L., Gunther, V., Dichtl, B., Georgiev, O., and Schaffner, W. (2012) Polyglutamine tracts as modulators of transcriptional activation from yeast to mammals. *Biol. Chem. 393*, 63−70.

(9) Sugiyama, S., and Tanaka, M. (2014) Self-propagating amyloid as a critical regulator for diverse cellular functions. *J. Biochem. 155*, 345−351.

(10) Gatchel, J. R., and Zoghbi, H. Y. (2005) Diseases of unstable repeat expansion: Mechanisms and common principles. *Nat. Rev. Genet. 6*, 743−755.

(11) Labbadia, J., and Morimoto, R. I. (2013) Huntington's disease: underlying molecular mechanisms and emerging concepts. *Trends Biochem. Sci. 38*, 378−385.

(12) Muralidharan, V., Oksman, A., Pal, P., Lindquist, S., and Goldberg, D. E. (2012) Plasmodium falciparum heat shock protein 110 stabilizes the asparagine repeat-rich parasite proteome during malarial fevers. *Nat. Commun. 3*, 1310−1310.

(13) Malinovska, L., Palm, S., Gibson, K., Verbavatz, J.-M., and Alberti, S. (2015) Dictyostelium discoideum has a highly Q/N-rich proteome and shows and unusual resilience to protein aggregation. *Proc. Natl. Acad. Sci. U. S. A. 112*, E2620−E2629.

(14) Halfmann, R., Alberti, S., Krishnan, R., Lyle, N., O'Donnell, C. W., King, O. D., Berger, B., Pappu, R. V., and Lindquist, S. (2011) Opposing effects of glutamine and asparagine govern prion formation by intrinsically disordered proteins. *Mol. Cell 43*, 72−84.

(15) Peters, T. W., and Huang, M. X. (2007) Protein aggregation and polyasparagine-mediated cellular toxicity in Saccharomyces cerevisiae. *Prion 1*, 144−153.

(16) Salazar, A. M., Silverman, E. J., Menon, K. P., and Zinn, K. (2010) Regulation of synaptic pumilio function by an aggregation-prone domain. *J. Neurosci. 30*, 515−522.

(17) Perutz, M. F., Pope, B. J., Owen, D., Wanker, E. E., and Scherzinger, E. (2002) Aggregation of proteins with expanded glutamine and alanine repeats of the glutamine-rich and asparagine-rich domains of Sup35 and of the amyloid beta-peptide of amyloid plaques. *Proc. Natl. Acad. Sci. U. S. A. 99*, 5596−5600.

(18) Chen, S. M., Ferrone, F. A., and Wetzel, R. (2002) Huntington's disease age-of-onset linked to polyglutamine aggregation nucleation. *Proc. Natl. Acad. Sci. U. S. A. 99*, 11884−11889.

(19) Chen, S. M., Berthelier, V., Hamilton, J. B., O'Nuallai, B., and Wetzel, R. (2002) Amyloid-like features of polyglutamine aggregates and their assembly kinetics. *Biochemistry 41*, 7391−7399.

(20) Walters, R. H., and Murphy, R. M. (2009) Examining polyglutamine peptide length: A connection between collapsed conformations and increased aggregation. *J. Mol. Biol. 393*, 978−992.

(21) Singh, V. R., and Lapidus, L. J. (2008) The intrinsic stiffness of polyglutamine peptides. *J. Phys. Chem. B 112*, 13172−13176.

(22) Crick, S. L., Ruff, K. M., Garai, K., Frieden, C., and Pappu, R. V. (2013) Unmasking the roles of N- and C-terminal flanking sequences from exon 1 of huntingtin as modulators of polyglutamine aggregation. *Proc. Natl. Acad. Sci. U. S. A. 110*, 20075−20080.

(23) Lu, X. M., and Murphy, R. M. (2014) Synthesis and disaggregation of asparagine repeat-containing peptides. *J. Pept. Sci. 20*, 860−867.

(24) Conchillo-Sole, O., de Groot, N. S., Aviles, F. X., Vendrell, J., Daura, X., and Ventura, S. (2007) AGGRESCAN: a server for the prediction and evaluation of "hot spots" of aggregation in polypeptides. *BMC Bioinf. 8*, 65−82.

(25) Garbuzynskiy, S. O., Lobanov, M. Y., and Galzitskaya, O. V. (2010) FoldAmyloid: a method of prediction of amyloidogenic regions from protein sequence. *Bioinformatics 26*, 326−332.

(26) Linding, R., Schymkowitz, J., Rousseau, F., Diella, F., and Serrano, L. (2004) A comparative study of the relationship between protein structure and beta-aggregation in globular and intrinsically disordered proteins. *J. Mol. Biol. 342*, 345−353.

(27) Fernandez-Escamilla, A. M., Rousseau, F., Schymkowitz, J., and Serrano, L. (2004) Prediction of sequence-dependent and mutational effects on the aggregation of peptides and proteins. *Nat. Biotechnol. 22*, 1302−1306.

(28) Dubay, K. F., Pawar, A. P., Chiti, F., Zurdo, J., Dobson, C. M., and Vendruscolo, M. (2004) Prediction of the absolute aggregation rates of amyloidogenic polypeptide chains. *J. Mol. Biol. 341*, 1317−1326.

(29) Walters, R. H., and Murphy, R. M. (2011) Aggregation kinetics of interrupted polyglutamine peptides. *J. Mol. Biol. 412*, 505−519.

(30) Perczel, A., Hollosi, M., Foxman, B. M., and Fasman, G. D. (1991) Conformational-analysis of pseudocyclic hexapeptides based on quantitative circular-dichroism (CD), NOE, and X-Ray Data - the Pure Cd Spectra of Type-I and Type-Ii Beta-Turns. *J. Am. Chem. Soc. 113*, 9772−9784.

(31) Zhang, Y., and Sagui, C. (2015) Secondary structure assignment for conformationally irregular peptides: Comparison between DSSP, STRIDE and KAKSI. *J. Mol. Graphics Modell. 55*, 72−84.

(32) Yang, D. T., Lu, X. M., Fan, Y. M., and Murphy, R. M. (2014) Evaluation of nanoparticle tracking for characterization of fibrillar protein aggregates. *AIChE J. 60*, 1236−1244.

(33) Filipe, V., Hawe, A., and Jiskoot, W. (2010) Critical evaluation of Nanoparticle Tracking Analysis (NTA) by NanoSight for the measurement of nanoparticles and protein aggregates. *Pharm. Res. 27*, 796−810.

(34) Kar, K., Jayaraman, M., Sahoo, B., Kodali, R., and Wetzel, R. (2011) Critical nucleus size for disease-related polyglutamine aggregation is repeat-length dependent. *Nat. Struct. Mol. Biol. 18*, 328−336.

(35) Landrum, E., and Wetzel, R. (2014) Biophysical underpinnings of the repeat length dependence of polyglutamine amyloid formation. *J. Biol. Chem. 289*, 10254−10260.

(36) Slepko, N., Bhattacharyya, A. M., Jackson, G. R., Steffan, J. S., Marsh, J. L., Thompson, L. M., and Wetzel, R. (2006) Normal-repeat-length polyglutamine peptides accelerate aggregation nucleation and cytotoxicity of expanded polyglutamine proteins. *Proc. Natl. Acad. Sci. U. S. A. 103*, 14367−14372.

(37) Klingstedt, T., Aslund, A., Simon, R. A., Johansson, L. B. G., Mason, J. J., Nystrom, S., Hammarstrom, P., and Nilsson, K. P. R. (2011) Synthesis of a library of oligothiophenes and their utilization as fluorescent ligands for spectral assignment of protein aggregates. *Org. Biomol. Chem. 9*, 8356−8370.

(38) Biancalana, M., and Koide, S. (2010) Molecular mechanism of Thioflavin-T binding to amyloid fibrils. *Biochim. Biophys. Acta, Proteins Proteomics 1804*, 1405−1412.

(39) Goransson, A. L., Nilsson, K. P. R., Kagedal, K., and Brorsson, A. C. (2012) Identification of distinct physiochemical properties of toxic prefibrillar species formed by A beta peptide variants. *Biochem. Biophys. Res. Commun. 420*, 895−900.

DOI: 10.1021/acs.biochem.5b00644
Biochemistry 2015, 54, 4784−4794

(40) Halfmann, R. L. S., and Lindquist, S. (2008) Screening for amyloid aggregation by semi-denaturing detergent-agarose gel electrophoresis. *J. Visualized Exp. 17*, 838.
(41) Kushnirov, V. V., Alexandrov, I. M., Mitkevich, O. V., Shkundina, I. S., and Ter-Avanesyan, M. D. (2006) Purification and analysis of prion and amyloid aggregates. *Methods 39*, 50−55.
(42) Wolfenden, R., Andersson, L., Cullis, P. M., and Southgate, C. C. B. (1981) Affinities of amino-acid side-chains for solvent water. *Biochemistry 20*, 849−855.
(43) Rhys, N. H., Soper, A. K., and Dougan, L. (2012) The hydrogen-bonding ability of the amino acid glutamine revealed by neutron diffraction experiments. *J. Phys. Chem. B 116*, 13308−13319.
(44) Crick, S. L., Jayaraman, M., Frieden, C., Wetzel, R., and Pappu, R. V. (2006) Fluorescence correlation spectroscopy shows that monomeric polyglutamine molecules form collapsed structures in aqueous solutions. *Proc. Natl. Acad. Sci. U. S. A. 103*, 16764−16769.
(45) Dougan, L., Li, J. Y., Badilla, C. L., Berne, B. J., and Fernandez, J. M. (2009) Single homopolypeptide chains collapse into mechanically rigid conformations. *Proc. Natl. Acad. Sci. U. S. A. 106*, 12605−12610.
(46) Vitalis, A., Lyle, N., and Pappu, R. V. (2009) Thermodynamics of beta-sheet formation in polyglutamine. *Biophys. J. 97*, 303−311.
(47) Vitalis, A., and Pappu, R. V. (2011) Assessing the contribution of heterogeneous distributions of oligomers to aggregation mechanisms of polyglutamine peptides. *Biophys. Chem. 159*, 14−23.
(48) Walters, R. H., Jacobson, K. H., Pedersen, J. A., and Murphy, R. M. (2012) Elongation kinetics of polyglutamine peptide fibrils: A quartz crystal microbalance with dissipation study. *J. Mol. Biol. 421*, 329−347.
(49) Dunker, A. K., Lawson, J. D., Brown, C. J., Williams, R. M., Romero, P., Oh, J. S., Oldfield, C. J., Campen, A. M., Ratliff, C. R., Hipps, K. W., Ausio, J., Nissen, M. S., Reeves, R., Kang, C. H., Kissinger, C. R., Bailey, R. W., Griswold, M. D., Chiu, M., Garner, E. C., and Obradovic, Z. (2001) Intrinsically disordered protein. *J. Mol. Graphics Modell. 19*, 26−59.
(50) Dyson, H. J. (2011) Expanding the proteome: disordered and alternatively folded proteins. *Q. Rev. Biophys. 44*, 467−518.
(51) Dyson, H. J., and Wright, P. E. (2005) Intrinsically unstructured proteins and their functions. *Nat. Rev. Mol. Cell Biol. 6*, 197−208.
(52) Turoverov, K. K., Kuznetsova, I. M., and Uversky, V. N. (2010) The protein kingdom extended: Ordered and intrinsically disordered proteins, their folding, supramolecular complex formation, and aggregation. *Prog. Biophys. Mol. Biol. 102*, 73−84.
(53) Schaefer, M. H., Wanker, E. E., and Andrade-Navarro, M. A. (2012) Evolution and function of CAG/polyglutamine repeats in protein-protein interaction networks. *Nucleic Acids Res. 40*, 4273−4287.
(54) Pratt, W. B., Gestwicki, J. E., Osawa, Y., and Lieberman, A. P. (2015) Targeting Hsp90/Hsp70-Based protein quality control for treatment of adult onset neurodegenerative diseases. *Annu. Rev. Pharmacol. Toxicol. 55*, 353−371.
(55) Arrasate, M., Mitra, S., Schweitzer, E. S., Segal, M. R., and Finkbeiner, S. (2004) Inclusion body formation reduces levels of mutant huntingtin and the risk of neuronal death. *Nature 431*, 805−810.
(56) Nekooki-Machida, Y., Kurosawa, M., Nukina, N., Ito, K., Oda, T., and Tanaka, M. (2009) Distinct conformations of in vitro and in vivo amyloids of huntingtin-exon1 show different cytotoxicity. *Proc. Natl. Acad. Sci. U. S. A. 106*, 9679−9684.
(57) Olshina, M. A., Angley, L. M., Ramdzan, Y. M., Tang, J. W., Bailey, M. F., Hill, A. F., and Hatters, D. M. (2010) Tracking mutant Huntingtin aggregation kinetics in cells reveals three major populations that include an invariant oligomer pool. *J. Biol. Chem. 285*, 21807−21816.
(58) Newby, G. A., and Lindquist, S. (2013) Blessings in disguise: biological benefits of prion-like mechanisms. *Trends Cell Biol. 23*, 251−259.

DOI: 10.1021/acs.biochem.5b00644
Biochemistry 2015, 54, 4784−4794